Ultrasound-Assisted Liposuction Does Not Compromise the Regenerative Potential of Adipose-Derived Stem Cells

DOMINIK DUSCHER,[a,b,c,*] DAVID ATASHROO,[a,*] ZESHAAN N. MAAN,[a] ANNA LUAN,[a] ELIZABETH A. BRETT,[a] JANOS BARRERA,[a] SACHA M. KHONG,[a] ELIZABETH R. ZIELINS,[a] ALEXANDER J. WHITTAM,[a] MICHAEL S. HU,[a] GRAHAM G. WALMSLEY,[a,d] MICHAEL S. POLLHAMMER,[b] MANFRED SCHMIDT,[b] ARNDT F. SCHILLING,[c] HANS-GÜNTHER MACHENS,[c] GEORG M. HUEMER,[b] DERRICK C. WAN,[a] MICHAEL T. LONGAKER,[a,d] GEOFFREY C. GURTNER[a]

[a]Hagey Laboratory for Pediatric Regenerative Medicine, Division of Plastic Surgery, and [d]Institute for Stem Cell Biology and Regenerative Medicine, School of Medicine, Stanford University, Stanford, California, USA; [b]Section of Plastic, Aesthetic and Reconstructive Surgery, Johannes Kepler University, Linz, Austria; [c]Department of Plastic Surgery and Hand Surgery, Technical University Munich, Munich, Germany

*Contributed equally.

Correspondence: Geoffrey C. Gurtner, M.D., Stanford University School of Medicine, 257 Campus Drive, Stanford, California 94305, USA. Telephone: 650-736-2776; E-Mail: ggurtner@stanford.edu

ABSTRACT

Human mesenchymal stem cells (MSCs) have recently become a focus of regenerative medicine, both for their multilineage differentiation capacity and their excretion of proregenerative cytokines. Adipose-derived mesenchymal stem cells (ASCs) are of particular interest because of their abundance in fat tissue and the ease of harvest via liposuction. However, little is known about the impact of different liposuction methods on the functionality of ASCs. Here we evaluate the regenerative abilities of ASCs harvested via a third-generation ultrasound-assisted liposuction (UAL) device versus ASCs obtained via standard suction-assisted lipoaspiration (SAL). Lipoaspirates were sorted using fluorescent assisted cell sorting based on an established surface-marker profile (CD34+/CD31−/CD45−), to obtain viable ASCs. Yield and viability were compared and the differentiation capacities of the ASCs were assessed. Finally, the regenerative potential of ASCs was examined using an in vivo model of tissue regeneration. UAL- and SAL-derived samples demonstrated equivalent ASC yield and viability, and UAL ASCs were not impaired in their osteogenic, adipogenic, or chondrogenic differentiation capacity. Equally, quantitative real-time polymerase chain reaction showed comparable expression of most osteogenic, adipogenic, and key regenerative genes between both ASC groups. Cutaneous regeneration and neovascularization were significantly enhanced in mice treated with ASCs obtained by either UAL or SAL compared with controls, but there were no significant differences in healing between cell-therapy groups. We conclude that UAL is a successful method of obtaining fully functional ASCs for regenerative medicine purposes. Cells harvested with this alternative approach to liposuction are suitable for cell therapy and tissue engineering applications. STEM CELLS TRANSLATIONAL MEDICINE 2016;5:248–257

SIGNIFICANCE

Adipose-derived mesenchymal stem cells (ASCs) are an appealing source of therapeutic progenitor cells because of their multipotency, diverse cytokine profile, and ease of harvest via liposuction. Alternative approaches to classical suction-assisted liposuction are gaining popularity; however, little evidence exists regarding the impact of different liposuction methods on the regenerative functionality of ASCs. Human ASC characteristics and regenerative capacity were assessed when harvested via ultrasound-assisted (UAL) versus standard suction-assisted liposuction. ASCs obtained via UAL were of equal quality when directly compared with the current gold standard harvest method. UAL is an adjunctive source of fully functional mesenchymal stem cells for applications in basic research and clinical therapy.

INTRODUCTION

Mesenchymal stem cells (MSCs) have recently emerged as a promising therapeutic agent because of their multilineage differentiation capacity, utility in tissue engineering applications, and paracrine support of tissue repair [1, 2]. Successful tissue healing depends on a sufficient response to tissue injury and ischemia [3]. MSCs applied to a site of injury are able to provide regenerative growth factors and cytokines, as well as function as cellular building blocks for repair [4]. The regenerative potential of MSCs can further be enhanced by using biomimetic scaffolds for their application [5, 6].

Adipose-derived mesenchymal stem cells (ASCs) are a particularly interesting source for MSC-based therapy, because of their relative abundance and ease of harvest from adipose tissue [7]. Moreover, ASCs have the ability to proliferate rapidly and secrete high levels of proregenerative factors [8]. Encouraging pilot studies using human ASCs in vivo have confirmed their ability to heal calvarial defects [9], as well as enhance vascularization of composite ischemic tissue [10]. ASCs have several key advantages over other MSC populations, such as bone marrow-derived MSCs (BM-MSCs), including the decreasing number of BM-MSCs available with age, the large volumes of bone marrow required, and the procedural risks associated with bone marrow harvest [8, 11–13].

Liposuction is a safe and reliable method of obtaining ASCs, but little is known about the effects of different liposuction techniques on the regenerative abilities of ASCs. A new approach to lipoaspiration, ultrasound-assisted liposuction (UAL), is gaining popularity for its ability to improve the process of lipoaspiration, by decreasing blood loss and tissue trauma [14]. During UAL, a specialized probe or cannula is used that transmits ultrasound vibrations into the fat tissue [15]. The vibrations lead to emulsification of the fat, making it easier to remove [16]. It has been demonstrated that UAL-derived lipoaspirates contain viable adipocytes and can be successfully used as fat grafts [17, 18]. However, certain lipoaspiration methods can have detrimental effects on ASCs [19] and little evidence exists regarding the impact of UAL on harvested ASCs. Here we sought to determine whether harvesting via UAL compromises ASC plasticity and functionality. After assessment of cell yield, viability, and metabolic activity, we characterized the differentiation abilities of UAL- and SAL-derived ASCs via osteogenic, adipogenic, and chondrogenic induction in vitro. Next, we examined the regenerative gene expression of these cells and specifically determined their ability to support neovascularization and cutaneous regeneration in vivo. Collectively, this represents, to our knowledge, the first comprehensive and independent investigation of the functionality of UAL-derived ASCs and their utility in regenerative medicine.

MATERIALS AND METHODS

Human ASC Isolation and Flow Cytometric Analysis

Human lipoaspirates were collected from healthy, adult, female patients with approval from the Stanford University institutional review board. Paired specimens were collected using UAL and SAL. Two lipoaspirate samples were harvested from identical sites in each patient, with SAL being performed before UAL. SAL was performed using 3.0- to 5.0-mm hollow aspiration cannulas and UAL was performed using a VASER Lipo system (Solta Medical, Hayward, CA, http://www.solta.com) with the following parameters: 2.9- to 3.7-mm solid probes delivered energy at a vibration frequency of 36,000 Hz and a wave amplitude ranging from 71 to 76 μm, translating into 5–12 W of vibratory power [20].

ASCs were isolated from samples of 3 patients who were between the ages 28 and 48 years, had no medical comorbidities, and were undergoing elective liposuction of the abdomen, as described previously [7]. Briefly, raw lipoaspirates were washed and treated with 0.075% collagenase type I (Sigma-Aldrich, St. Louis, MO, http://www.sigmaaldrich.com) in Hanks' balanced salt solution (Cellgro, Manassas, VA, http://www.cellgro.com) for 1 hour at 37°C in a water bath with gentle agitation at 125 rpm. The collagenase digest was then inactivated by adding an equal volume of standard cell culture growth medium (Dulbecco's modified Eagle's medium (DMEM) plus GlutaMAX [Invitrogen, Carlsbad, CA, http://www.invitrogen.com], 10% fetal bovine serum, and 1% penicillin/streptomycin). The stromal vascular fraction (SVF) was pelleted by centrifugation at 300g for 5 minutes. The supernatant was then discarded, and the cell pellet was resuspended and filtered through a 100-μm cell strainer to remove undigested tissue fragments. The cells were pelleted, resuspended, and then fluorescence-activated cell sorting (FACS) was used to obtain ASCs (defined as the CD45−/CD31−/CD34+ cell fraction) using the following mouse anti-human monoclonal antibodies: CD31-PE, CD45-PeCy7, and CD34-APC (BD Biosciences, San Jose, CA, http://www.bdbiosciences.com). This surface-marker profile was chosen to exclude hematopoietic and endothelial cells, and was used in combination with propidium iodide to eliminate dead cells [21]. FACS was performed using a BD FACSAria cell sorter (BD Biosciences, San Jose, CA).

In Vitro ASC Metabolic Activity

Viability was compared between pooled ASCs freshly isolated via FACS from UAL and SAL lipoaspirates (n = 3) using an MTT assay for metabolic activity according to manufacturer's instructions (Vybrant MTT Cell Proliferation Assay Kit; Invitrogen). Cells were seeded into 96-well plates at a density of 20,000 cells per well in culture medium. Plates were incubated at 37°C and 5% CO_2, and cellular metabolism was evaluated over 7 days. The absorbance of each well was determined using a microplate reader at 540 nm (SpectraMAX 384 Plus; Molecular Devices Ltd., Sunnyvale, CA, http://www.moleculardevices.com). All assays were done in triplicate.

In Vitro Osteogenic Differentiation

Pooled ASCs freshly isolated via FACS from UAL and SAL lipoaspirates (n = 3) were seeded in standard 6-well tissue culture plates (1.0 $\times$ 10^5 cells per well) in triplicate and grown to at least 80% confluence before being exposed to osteogenic differentiation medium, which consisted of DMEM (1 g/l glucose) supplemented with 10% fetal bovine serum, 1% penicillin/streptomycin, 100 μg/ml ascorbic acid, and 10 mM β-glycerophosphate. Alizarin red staining was performed and quantified after 14 days to assay extracellular mineralization, as previously described [19, 22]. Briefly, cells stained with Alizarin red were incubated with 2 ml of a solution of 20% methanol and 10% acetic acid under gentle shaking for 15 minutes at room temperature. Absorption of samples was measured at 450 nm using an Ultraspec 2100 Pro spectrophotometer (Biochrom Ltd., Cambridge, U.K., http://www.biochrom.co.uk). Staining of all samples was performed in triplicate, and all measurements were normalized to the total protein content of a sister well seeded at equal density. Photometric quantification of alkaline phosphatase staining was performed after 7 days. ImageJ software (National Institutes of Health, Bethesda, MD, http://www.nih.gov) was used to binarize images taken with the same microscope settings. Intensity threshold values were set automatically and quantification of staining was determined by pixel-positive area per high-power field, as previously described [5]. Finally, gene expression of the osteogenic markers runt-related-transcription factor-2 (RUNX2), osteopontin (OPN), and osteocalcin (OCN) was analyzed after

14 days of differentiation by quantitative real-time polymerase chain reaction (qRT-PCR).

In Vitro Adipogenic Differentiation

For adipogenic differentiation, pooled ASCs freshly isolated via FACS from UAL and SAL lipoaspirates (n = 3) were seeded in triplicate into standard 6-well tissue culture plates (1.5×10^5 cells per well), and adipogenic differentiation medium consisting of DMEM (1 g/l glucose), 10% fetal bovine serum, 1% penicillin/streptomycin, 10 μg/ml insulin, 1 μM dexamethasone, 0.5 mM methylxanthine, and 200 μM indomethacin was added after cell attachment. Oil Red O staining was performed after 7 days of incubation and photometrically quantified analog to alkaline phosphatase staining (described in the previous section). Finally, expression levels of the adipogenic genes peroxisome proliferator-activated receptor γ (PPAR-γ), fatty acid binding protein 4 (FABP4), and lipoprotein lipase (LPL) were examined at day 7 of differentiation by qRT-PCR.

In Vitro Chondrogenic Differentiation

Chondrogenic differentiation was performed using a commercially available kit (StemPro Chondrogenesis Differentition Kit; Life Technologies, CA, USA, http://www.thermofisher.com) per manufacturer protocol. Pooled ASCs freshly isolated via FACS from UAL and SAL lipoaspirates (n = 3) were resuspended in a dense cell solution of 1.6×10^7 cells/ml, using fully supplemented media. A 5-μl aliquot of the cell suspension was cultured in high humidity conditions for 2 hours (n = 3). Subsequently, chondrogenic differentiation medium was added to each well containing the cellular micromass, and cultured for 2 weeks. Cell nodules were then processed for cryosectioning, and were sectioned and histologically stained for glycosaminoglycans, using Alcian blue. Stained tissue was imaged at $\times 10$ magnification.

In Vitro Real-Time Quantitative PCR Analysis

Total RNA was harvested from cultivated cells using the RNeasy Mini Kit (Qiagen, Valencia, CA, http://www.qiagen.com) according to the manufacturer's protocol. Reverse transcription was performed and osteogenic, adipogenic, and regenerative gene expression was examined by qRT-PCR using the Prism 7900HT sequence detection system (Applied Biosystems, Foster City, CA, http://www.appliedbiosystems.com) and SYBR Green PCR Master Mix (Applied Biosystems). The amount of PCR product was calculated using an external glyceraldehyde-3-phosphate dehydrogenase (GAPDH) standard curve and LightCycler software (Roche Diagnostics, Indianapolis, IN, https://lifescience.roche.com). All values were normalized on the basis of the GAPDH expression in the corresponding samples. All experiments were performed in triplicate. Specific primers for the genes examined were based on their PrimerBank sequences (http://pga.mgh.harvard.edu/primerbank) [19].

Animals

All mice were housed in the Stanford University Veterinary Service Center in accordance with National Institutes of Health and institution-approved animal care guidelines. All procedures were approved by the Stanford University Administrative Panel on Laboratory Animal Care.

In Vivo Excisional Wound Model

Eight 12-week-old nude male Crl:CD-1-Foxn1^v mice (Charles River Laboratories, Wilmington, MA, http://www.criver.com) were randomized to 3 treatment groups: unseeded hydrogel control or hydrogel seeded with pooled human ASCs freshly isolated via FACS from UAL and SAL lipoaspirates from 3 donors. Pullulan-collagen hydrogel was produced as described previously [5]. To achieve capillary seeding, 2.5×10^5 human ASCs suspended in 15 μl of phosphate-buffered saline (PBS) solution was pipetted onto hydrophobic wax paper and the hydrogel was immediately placed on top. Cells were absorbed actively into the pores of the scaffold by capillary, hydrophobic, and entropic forces [6]. As previously described [23], two 6-mm, full-thickness wounds per mouse were excised from either side of the midline. Each wound was held open by donut-shaped silicone rings fastened with 6-0 nylon sutures to prevent wound contraction. For mice in the unseeded hydrogel control group, a 6-mm piece of hydrogel saturated with PBS was placed in each wound bed. For mice in the ASC-seeded hydrogel groups, a 6-mm piece of hydrogel seeded by capillary force with human ASCs (suspended in PBS) was placed in the wound bed. All wounds were covered with an occlusive dressing (Tegaderm; 3M, St. Paul, MN, http://www.3m.com). Digital photographs were taken on days 0, 3, 5, 7, 9, 11, 13, and 15. Wound area was measured using ImageJ software (National Institutes of Health) (n = 8 wounds per group).

Assessment of Wound Vascularity

Vascularity of healed wounds was assessed by immunohistochemical staining for the endothelial cell marker CD31 (n = 8 wounds per condition). Briefly, wounds from the excisional model were harvested upon closure and processed for paraffin sectioning. Immunohistochemical staining of 7-μm-thick paraffin sections for CD31 was used to quantify wound vascularity, as described previously [5]. Briefly, slides were deparaffinized, washed in PBS, and blocked in a humidified chamber for 2 hours. Primary antibody (1:100 Rb α CD31, Ab28364; Abcam, Cambridge, U.K., http://www.abcam.com) was incubated overnight at 4°C, followed by secondary antibody staining (1:400 AF547 Gt α Rb; Life Technologies, Grand Island, NY, http://www.lifetechnologies.com). Cell nuclei were visualized with the nuclear stain 4′,6-diamidino-2-phenylindole (DAPI). ImageJ software (National Institutes of Health) was used to binarize immunofluorescent images taken with the same gain, exposure, and excitation settings, as previously described [5]. Intensity threshold values were set automatically and quantification of CD31 staining was determined by pixel-positive area per high-power field.

Statistical Analysis

All values are expressed as mean $\pm$ SEM. Statistical significance analyses were performed using a Student's t test or one-way analysis of variance were indicated. The probability of a type I error was set at $\alpha = 0.05$.

RESULTS

UAL Does Not Compromise ASC Yield, Viability or Metabolic Activity

Initially, we assessed whether UAL-based harvesting reduces ASC yield compared with SAL. On FACS analysis, we found the viability (supplemental online Fig. 1) and frequency of ASCs within adipose tissue (defined by the percentage of CD45−/CD31−/CD34+ cells within the SVF [24]) to be similar between groups (Fig. 1A, 1B).
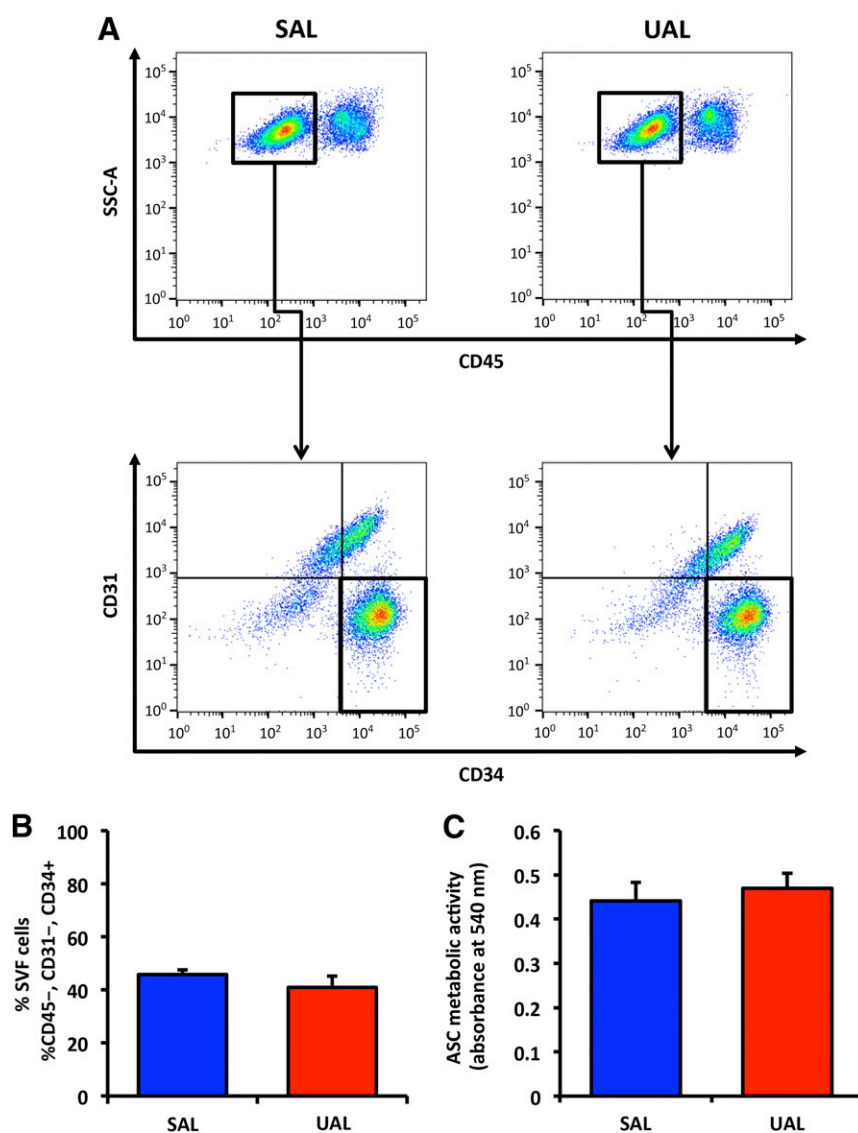
Figure 1. UAL and SAL lipoaspirates yield similar amounts of ASCs with comparable viability. **(A):** Flow cytometric analysis evaluating the percentage of CD45− cells (top row) and ASCs (CD45−/CD31−/CD34+ cells; bottom row) within the SVF from UAL and SAL lipoaspirates. **(B):** Quantification of CD45−/CD31−/CD34+ ASCs in UAL- and SAL-derived SVF revealed no significant difference in ASC yield across samples. **(C):** MTT assay demonstrated no significant difference in cellular metabolic activity. $n = 3$. All data are given as mean $\pm$ 1 SEM. Abbreviations: ASC, adipose-derived mesenchymal stem cell; SAL, suction-assisted liposuction; SVF, stromal vascular fraction; UAL, ultrasound-assisted liposuction.

ASC viability was 74% $\pm$ 4.8% for SAL and 76% $\pm$ 8.2% for UAL lipoaspirates. UAL lipoaspirates yielded a mean of 41% $\pm$ 4.2%, and the mean SAL lipoaspirate yield was 45% $\pm$ 1.7% ASCs. After having established that fat tissue harvested via UAL and SAL yielded comparable amounts of progenitor cells, we next examined the metabolic activity of isolated ASCs in vitro. Consistent with our FACS results on viability, no difference in ASC metabolic activity could be detected between UAL and SAL groups (Fig. 1C).

ASCs Harvested via UAL and SAL Have a Comparable Osteogenic Differentiation Capacity

ASCs are increasingly being studied for skeletal regenerative medicine applications [25]. Therefore, we characterized the osteogenic differentiation abilities of ASCs harvested either by SAL or UAL. Consistent with previous studies [22], we found that

osteogenic differentiation capacity was not impaired in ASCs harvested using third-generation ultrasound (Fig. 2). Examining alkaline phosphatase expression after 7 days in osteogenic culture conditions revealed no significant differences between the ASC groups (Fig. 2A). Investigating the mineralization of the extracellular matrix via Alizarin red staining on day 14 of osteogenic stimulation also demonstrated similar results across samples (Fig. 2B). Osteogenic induction of ASCs over 14 days not only resulted in phenotypic differentiation but also upregulation of osteogenic gene expression. We assessed the levels of the key osteogenic genes *RUNX2*, *OPN*, and *OCN* (Fig. 2C). Interestingly, although both *RUNX2* and *OCN* showed similar expression levels after 14 days of osteogenic stimulation, *OPN* was expressed at significantly higher levels in ASCs harvested via UAL ($p < .05$). This could imply that UAL-derived ASCs are an advantageous source for bone tissue engineering or therapeutic
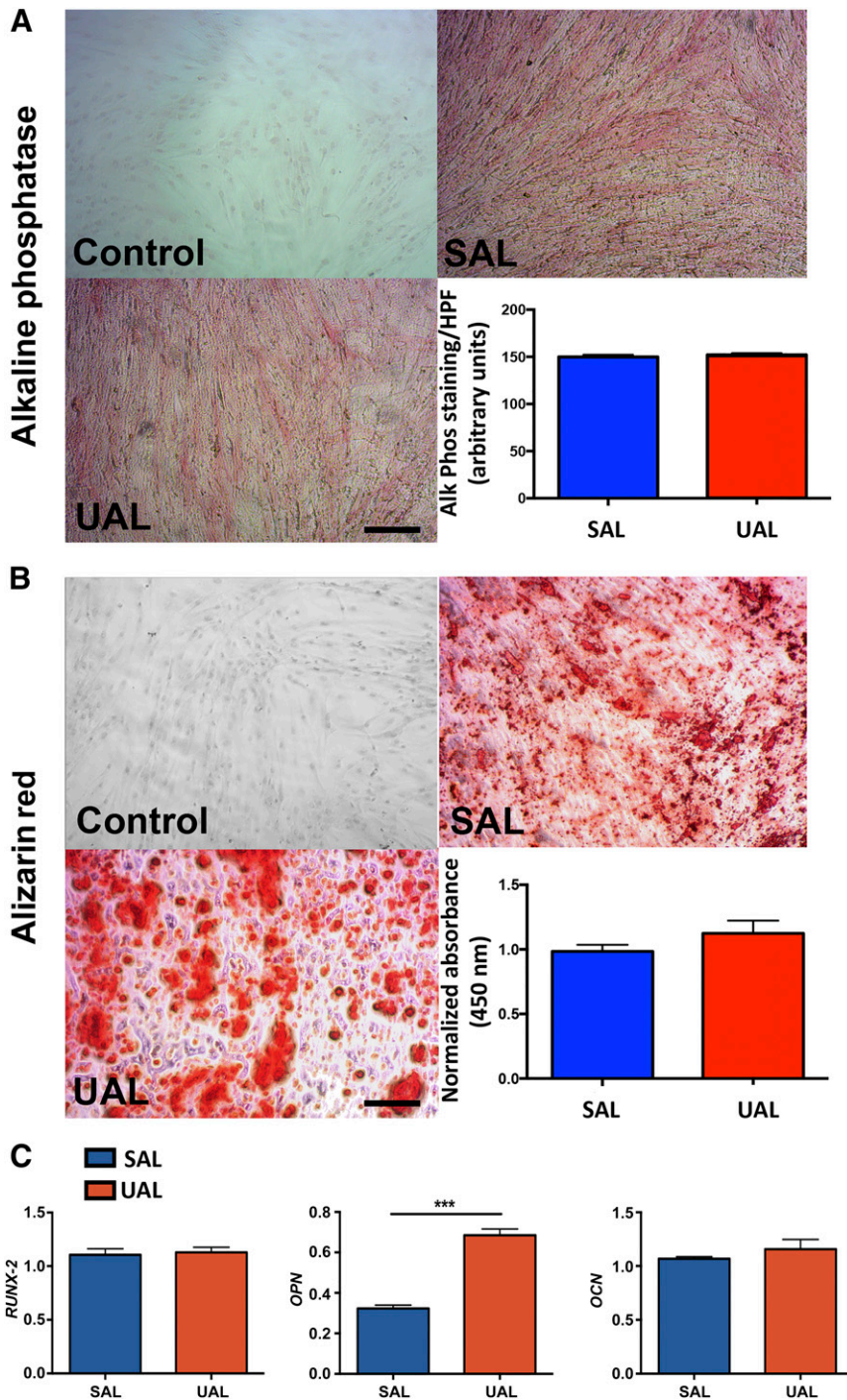
Figure 2. UAL- and SAL-derived adipose-derived mesenchymal stem cells (ASCs) have comparable osteogenic lineage differentiation capacities. **(A, B):** Representative images and quantification of alkaline phosphatase **(A)** and Alizarin red staining **(B)** following osteogenic differentiation of UAL- and SAL-derived ASCs. **(C):** Real-time polymerase chain reaction quantifying the expression of early (*RUNX2*), intermediate (*OPN*), and late (*OCN*) osteogenic markers in UAL versus SAL ASCs in vitro. Scale bars = 100 μm. *n* = 3. All data are given as mean $\pm$ 1 SEM. ∗∗∗, $p \leq$ .05. Abbreviations: Alk phos, alkaline phosphatase; HPF, high-power field; *OCN*, osteocalcin; *OPN*, osteopontin; Phos, phosphatase; *RUNX2*, runt-related transcription factor 2; SAL, suction-assisted liposuction; UAL, ultrasound-assisted liposuction.

approaches for bone regeneration. The minor morphological difference between ASCs harvested via UAL and SAL and the trend for increased mineralization in the UAL group (Fig. 2B) may be additional hints for a slightly improved osteogenic profile of these cells.

UAL and SAL Yield ASCs With Equal Adipogenic and Chondrogenic Differentiation Capacity
Next, we examined in vitro adipogenic and chondrogenic differentiation in ASCs harvested via UAL and SAL. Consistent with preserved stemness despite ultrasound exposure, UAL-harvested
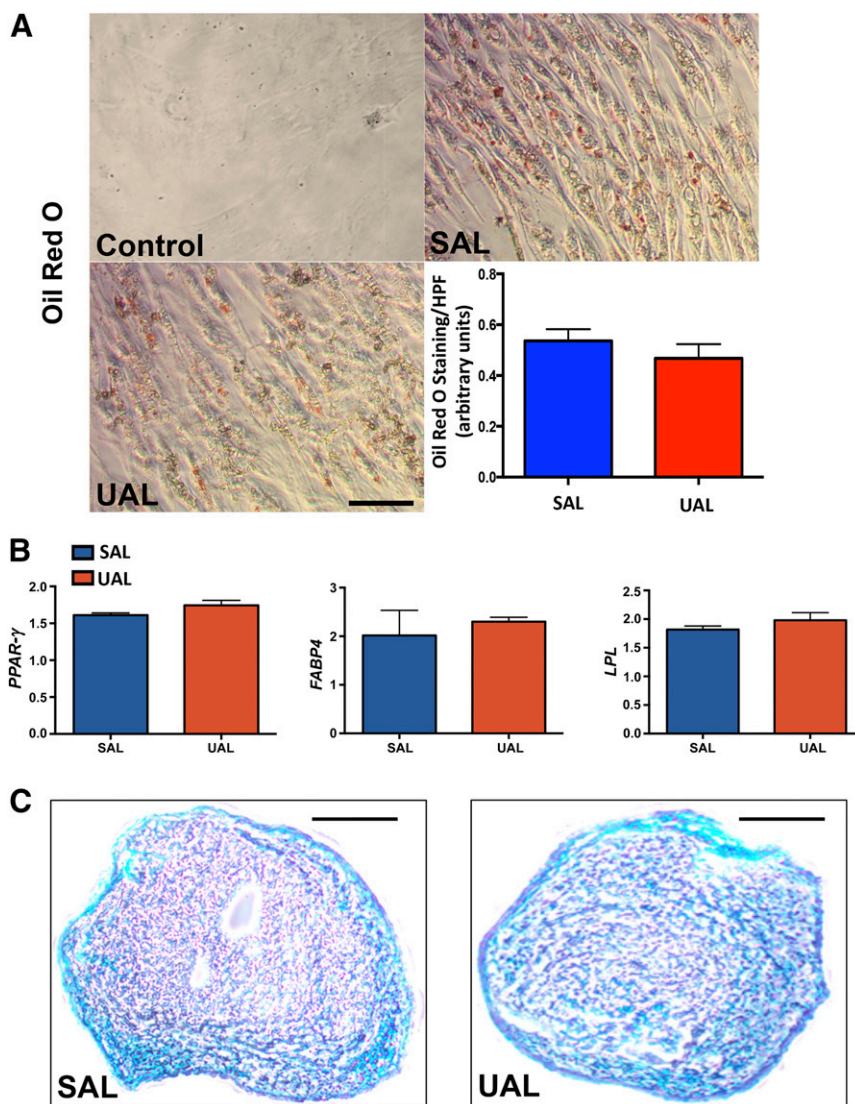
Figure 3. UAL- and SAL-derived adipose-derived mesenchymal stem cells (ASCs) have equal adipogenic and chondrogenic lineage differentiation capacities. **(A):** Representative images and quantification of Oil Red O staining following osteogenic differentiation of UAL and SAL derived ASCs. **(B):** Real-time polymerase chain reaction quantifying the expression of selected adipogenic markers in UAL versus SAL ASCs in vitro. Scale bar = 25 μm. **(C):** Representative images of cryosectioned cartilagenous nodules differentiated from UAL and SAL ASCs stained using Alcian blue. No gross or microscopic differences could be appreciated. Scale bars = 100 μm. n = 3. All data are given as mean $\pm$ 1 SEM. Abbreviations: *FABP4*, fatty acid binding protein 4; HPF, high-power field; *LPL*, lipoprotein lipase; *PPAR-γ*, peroxisome proliferator-activated receptor γ; SAL, suction-assisted liposuction; UAL, ultrasound-assisted liposuction.

ASCs differentiated into the adipogenic and chondrogenic lineage similar to ASCs harvested via SAL (Fig. 3). To characterize the adipogenic potential of ASCs, we first exposed them to adipogenic differentiation medium for 7 days in vitro before staining with Oil Red O. Comparing the staining intensity across groups revealed no significant difference between ASCs derived from UAL versus SAL lipoaspirates (Fig. 3A). Next, we compared the gene expression of key adipogenic markers, such as *PPAR-γ*, *FABP4*, and *LPL* on day 7 after adipogenic induction. In contrast to slight variations in osteogenic marker expression, no significant difference in adipogenic expression profiles could be detected between UAL- and SAL-derived ASCs (Fig. 3B). Additionally, ASCs differentiated from SAL and UAL groups exhibited histologically similar formation of cartilagenous extracellular matrix under chondrogenic differentiation on Alcian blue staining (Fig. 3C). In

aggregate, these data suggest that harvesting via UAL still allows adipogenic and chondrogenic differentiation of human ASCs.

UAL and SAL ASCs Have Similar Regenerative Growth Factor and Cytokine Expression Profiles

After assessing the plasticity of SAL and UAL ASCs, we next investigated the regenerative potential of these cells. Therefore, quantitative PCR (qPCR) was used to analyze gene expression of key regenerative cytokines and growth factors (Fig. 4). ASCs from SAL and UAL lipoaspirates were obtained using FACS, and collected for RNA processing. Comparison of relative gene expression levels revealed no significant differences between the groups for hepatocyte growth factor (*Hgf*), basic fibroblast growth factor-2 (*Fgf-2*), stromal cell-derived factor 1 (*Sdf-1*),
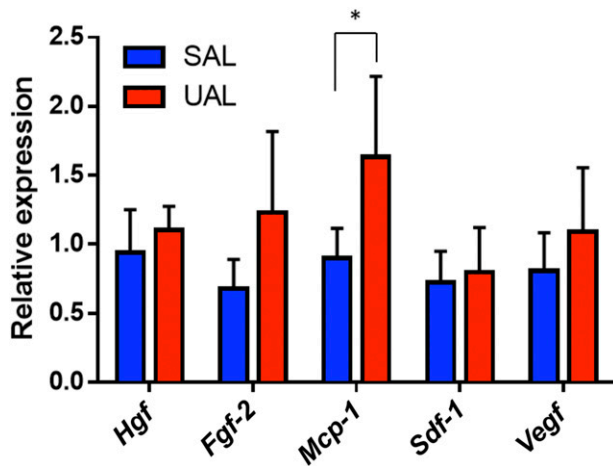
Figure 4. UAL and SAL adipose-derived mesenchymal stem cells (ASCs) display similar regenerative growth factor and cytokine expression. Quantitative polymerase chain reaction was used to analyze gene expression for five different regenerative growth factors and cytokines. ASCs harvested from SAL and UAL lipoaspirates demonstrated comparable expression levels of *Hgf*, *Fgf-2*, *Sdf-1*, and *Vegf*. A significant difference between the groups was detectable for Mcp-1. $n = 3$. All data are given as mean $\pm$ 1 SEM. ∗, $p \leq .05$. Abbreviations: *Hgf*, hepatocyte growth factor; *Fgf-2*, basic fibroblast growth factor; *Mcp-1*, monocyte chemotactic protein 1; SAL, suction-assisted liposuction; *Sdf-1*, stromal cell-derived factor 1; UAL, ultrasound-assisted liposuction; *Vegf*, vascular endothelial growth factor.

and vascular endothelial growth factor (*Vegf*). However, there was a significant difference in the expression of monocyte chemotactic protein 1 (*Mcp-1*) ($p < .05$), with higher levels in UAL ASCs suggesting a potential advantage of these cells in leukocyte chemotaxis [26].

Application of ASCs Harvested via UAL and SAL Enhances Wound Healing

Studies from our group and others have demonstrated the capacity of ASCs to support tissue repair in vivo [6, 27, 28]. To determine the therapeutic functionality of UAL-versus SAL-derived ASCs in vivo, cell-seeded hydrogels [6] were applied to a previously established model of murine cutaneous wound healing [6, 29] (Fig. 5). We found that ASCs obtained via UAL and SAL displayed equal therapeutic efficacy for cutaneous regeneration (Fig. 5A). Wounds treated with both UAL- and SAL-derived ASC-seeded hydrogels showed significantly improved healing rates as early as day 3 compared with unseeded hydrogel controls (Fig. 5B), and also had significantly faster wound closure times (11 and 11.6 days vs. 14.1 days; $p < .01$) (Fig. 5C). These findings suggest that ASCs harvested via both SAL and UAL are fully functional in therapeutic approaches for tissue cutaneous regeneration.

UAL- and SAL-Derived ASCs Enhance Wound Vascularity

Consistent with our results regarding in vivo regenerative functionality, healed wounds in both ASC treatment groups displayed significantly enhanced neovascularization compared with acellular scaffold controls ($p < .05$), with no significant differences between UAL and SAL groups (Fig. 6). These data confirm the comparable regenerative potential of ASCs harvested via SAL and UAL in vivo.

DISCUSSION

Stem cell research has led to remarkable advancements in the fields of tissue engineering and regenerative medicine. In particular, adult MSCs have garnered increasing interest for their positive impact on tissue repair [30]. MSCs have shown sufficient promise and safety in preclinical trials to warrant testing in human patients [31]. Despite the promise of MSC-based therapies, clinical translation has been slowed by the need to identify optimal cell sourcing, processing, and delivery techniques [2].

Although BM-MSCs have been studied more extensively, ASCs are an emerging stem cell population for basic science, as well as translational and clinical research [32]. ASCs have demonstrated efficacy in tissue engineering and regenerative medicine applications [33]. Specifically, we have shown successful treatment of critically sized calvarial defects in mice with ASC-seeded, apatite-coated, poly(lactic-coglycolic acid) scaffolds [9] and that ASC-seeded, pullulan-collagen biomimetic scaffolds accelerate murine cutaneous wound healing and increase neovascularization [6]. Importantly, while comparable in their therapeutic efficacy [34], ASCs possess a significant clinical advantage over BM-MSCs with regard to their relative abundance and ease of harvest from subcutaneous adipose tissue [35].

The increasing clinical demand for liposuction procedures is mirrored by the recent development of novel lipoaspiration methods such as suction- or power-assisted, laser-assisted, and ultrasound-assisted liposuction. These techniques were developed with the goal of achieving rapid tissue harvest, promoting skin tightening, and minimizing harvest-site morbidity [15]. The emergence of lipoaspirates as an important source of MSCs has led to research exploring the effects of different liposuction techniques on the harvested tissue. Given the wide variety of techniques available for use in clinical practice, this research is critically important to determine the suitability of tissue and cells derived from lipoaspirate samples for regenerative medicine purposes.

ASC viability is an important indicator of the damage inflicted on adipose tissue during harvest. Keck et al. have shown that SAL with 0.5-bar negative pressure leads to cell yield and viability comparable to manual lipoaspiration [36]. Alternatively, laser-assisted liposuction (LAL), which uses thermolysis to selectively lyse adipocytes, has been shown to decrease ASC yield and viability as compared with SAL [19]. In this study, we demonstrate that UAL, using pulsed ultrasound energy to selectively emulsify subcutaneous adipose tissue before aspiration [37], can be an effective method for harvesting ASCs with similar yield, viability, and metabolic activity as compared with SAL and, consequently, manual lipoaspiration. These data indicate the usefulness of UAL-derived lipoaspirates and cells in basic research and clinical applications.

The multilineage differentiation capacity of ASCs dictates their value for tissue engineering. LAL has been shown to inhibit ASC osteogenic gene induction and LAL-derived ASCs display impaired ability to heal murine calvarial defects in vivo [19]. In contrast, we found that OPN expression, an early marker of osteogenic differentiation [38], was increased in UAL-harvested ASCs as compared with those harvested by SAL. The slight increase of OPN expression could result in a subtle effect on early osteoblast development, which may lead to an advantage of UAL-derived ASCs in bone tissue engineering and healing. This
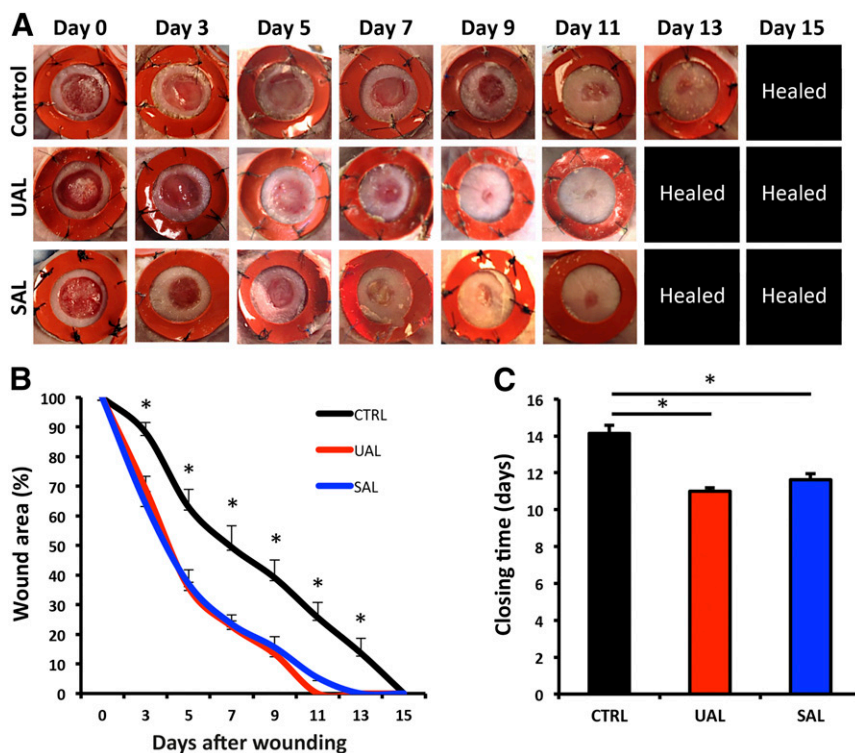
Figure 5. Application of adipose-derived mesenchymal stem cells (ASCs) harvested via UAL and SAL equally improve excisional wound healing. **(A–C):** Gross appearance **(A)**, wound healing kinetics **(B)**, and closing times **(C)** of humanized excisional murine wounds treated with hydrogel-seeded ASCs harvested via UAL or SAL, or unseeded hydrogel. $n = 8$. *, $p \leq .05$. All data are given as mean $\pm$ 1 SEM. Abbreviations: CTRL, control; SAL, suction-assisted liposuction; UAL, ultrasound-assisted liposuction.
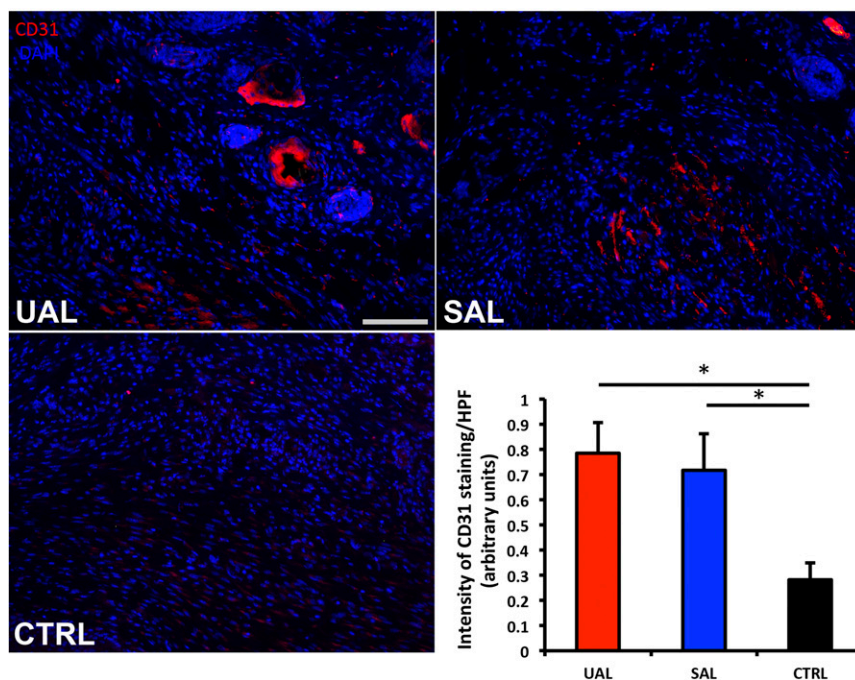

Figure 6. UAL- and SAL-derived hASC-seeded hydrogel groups improve cutaneous wound vascular density. CD31 staining with 4′,6-diamidino-2-phenylindole (DAPI) confirmed a significant increase in neovascularization among the hASC-seeded hydrogel groups. Scale bar = 100 μm. $n = 8$. *, $p \leq .05$. All data are given as mean $\pm$ 1 SEM. Abbreviations: CTRL, control; HPF, high-power field; SAL, suction-assisted liposuction; UAL, ultrasound-assisted liposuction.

warrants further research using specific assays. However, besides the minor alterations in expression profiles, no differences in the other in vitro assays for osteogenic differentiation potential could be detected and, from this study, we can conclude that both UAL- and SAL-derived ASCs are capable of osteogenic differentiation.

While previous studies have shown that SAL-derived ASCs have significantly higher expression levels of adipogenic differentiation markers [36], there were no significant differences between UAL- and SAL-derived ASCs' adipogenic gene expression profiles. Similarly, we could not detect any disadvantage for UAL-derived ASCs in a qualitative chondrogenic differentiation assay. These data suggest that UAL-harvested ASCs retain their multipotency and have comparable efficacy to SAL-derived ASCs for applications in tissue engineering. However, further in vivo studies are needed to confirm the full potential of UAL-harvested ASCs in hard and soft tissue engineering.

Increasingly, ASCs are studied for their enhancement of tissue regeneration [6]. Here, we show that UAL- and SAL-harvested ASCs have similar regenerative gene expression profiles and a comparable capacity for promoting cutaneous regeneration in a preclinical model of wound healing. Additionally, healed wounds treated with either UAL- or SAL-derived ASCs demonstrated significantly upregulated neovascularization compared with an unseeded-scaffold control group. These encouraging findings identify UAL as a new method for obtaining therapeutically efficacious MSCs.

CONCLUSION

In this study, we evaluated the effect of UAL on adipose-derived progenitor cell yield, viability, and functionality. We found that UAL-harvested lipoaspirates contain similar numbers of ASCs compared with SAL-derived samples. Furthermore, UAL-derived ASCs are equally viable and have similar differentiation capacities as SAL-harvested cells. Last, we could not show any

difference in therapeutic efficacy between UAL- and SAL-derived ASCs in an in vivo model of tissue regeneration. In aggregate, our data confirm UAL-derived lipoaspirates as a source of fully functional ASCs able to satisfy important criteria for stem cell applications in basic research and clinical therapy.

AUTHOR CONTRIBUTIONS

D.D.: conception and design, collection and/or assembly of data, manuscript writing, final approval of manuscript; D.A. and Z.N.M.: conception and design, collection and/or assembly of data; A.L., E.A.B., J.B., S.M.K., E.R.Z., A.J.W., M.S.H., and G.G.W.: collection and/or assembly of data; M.S.P. and M.S.: manuscript writing, final approval of manuscript; A.F.S., H-G.M., G.M.H., D.C.W., M.T.L., and G.C.G.: conception and design, manuscript writing, final approval of manuscript.

DISCLOSURE OF POTENTIAL CONFLICTS OF INTEREST

D.D. and G.C.G. are listed on the patent "Efficient Stem Cell Delivery Into Biomaterials Using a Novel Capillary Driven Encapsulation Technique" and G.C.G. is listed on the patent "Intelligent Biodegradable Pullulan Regenerative Matrix for Tissue Engineering" assigned to Stanford University. The other authors indicated no potential conflicts of interest.

REFERENCES

1 Caplan AI. Adult mesenchymal stem cells for tissue engineering versus regenerative medicine. J Cell Physiol 2007;213:341–347.

2 Wong VW, Sorkin M, Gurtner GC. Enabling stem cell therapies for tissue repair: Current and future challenges. Biotechnol Adv 2013; 31:744–751.

3 Gurtner GC, Werner S, Barrandon Y et al. Wound repair and regeneration. Nature 2008; 453:314–321.

4 Caplan AI, Dennis JE. Mesenchymal stem cells as trophic mediators. J Cell Biochem 2006;98:1076–1084.

5 Rustad KC, Wong VW, Sorkin M et al. Enhancement of mesenchymal stem cell angiogenic capacity and stemness by a biomimetic hydrogel scaffold. Biomaterials 2012;33:80–90.

6 Garg RK, Rennert RC, Duscher D et al. Capillary force seeding of hydrogels for adipose-derived stem cell delivery in wounds. STEM CELLS TRANSLATIONAL MEDICINE 2014;3:1079–1089.

7 Zuk PA, Zhu M, Ashjian P et al. Human adipose tissue is a source of multipotent stem cells. Mol Biol Cell 2002;13:4279–4295.

8 Nakanishi C, Nagaya N, Ohnishi S et al. Gene and protein expression analysis of mesenchymal stem cells derived from rat adipose tissue and bone marrow. Circ J 2011;75:2260–2268.

9 Levi B, James AW, Nelson ER et al. Human adipose derived stromal cells heal critical size mouse calvarial defects. PLoS One 2010;5:e11177.

10 Rehman J, Traktuev D, Li J et al. Secretion of angiogenic and antiapoptotic factors by human adipose stromal cells. Circulation 2004; 109:1292–1298.

11 Service RF. Tissue engineers build new bone. Science 2000;289:1498–1500.

12 Cowan CM, Shi YY, Aalami OO et al. Adipose-derived adult stromal cells heal critical-size mouse calvarial defects. Nat Biotechnol 2004;22:560–567.

13 De Ugarte DA, Morizono K, Elbarbary A et al. Comparison of multi-lineage cells from human adipose tissue and bone marrow. Cells Tissues Organs 2003;174:101–109.

14 Nagy MW, Vanek PF Jr. A multicenter, prospective, randomized, single-blind, controlled clinical trial comparing VASER-assisted Lipoplasty and suction-assisted Lipoplasty. Plast Reconstr Surg 2012;129:681e–689e.

15 Shridharani SM, Broyles JM, Matarasso A. Liposuction devices: Technology update. Med Devices (Auckl) 2014;7:241–251.

16 Cimino WW. The physics of soft tissue fragmentation using ultrasonic frequency vibration of metal probes. Clin Plast Surg 1999;26: 447–461.

17 Schafer ME, Hicok KC, Mills DC et al. . Aesthet Surg J 2013;33:698–704.

18 Fisher C, Grahovac TL, Schafer ME et al. Comparison of harvest and processing techniques for fat grafting and adipose stem cell isolation. Plast Reconstr Surg 2013;132:351–361.

19 Chung MT, Zimmermann AS, Paik KJ et al. Isolation of human adipose-derived stromal cells using laser-assisted liposuction and their therapeutic potential in regenerative medicine. STEM CELLS TRANSLATIONAL MEDICINE 2013;2:808–817.

20 Cimino WW. Ultrasonic surgery: Power quantification and efficiency optimization. Aesthet Surg J 2001;21:233–241.

21 Duscher D, Rennert RC, Januszyk M et al. Aging disrupts cell subpopulation dynamics and diminishes the function of mesenchymal stem cells. Sci Rep 2014;4:7144.

22 Panetta NJ, Gupta DM, Kwan MD et al. Tissue harvest by means of suction-assisted or third-generation ultrasound-assisted lipoaspiration has no effect on osteogenic potential of human adipose-derived stromal cells. Plast Reconstr Surg 2009;124:65–73.

23 Wong VW, Rustad KC, Glotzbach JP et al. Pullulan hydrogels improve mesenchymal stem cell delivery into high-oxidative-stress wounds. Macromol Biosci 2011;11:1458–1466.

24 Suga H, Matsumoto D, Eto H et al. Functional implications of CD34 expression in human adipose-derived stem/progenitor cells. Stem Cells Dev 2009;18:1201–1210.

25 Levi B, Longaker MT. Concise review: Adipose-derived stromal cells for skeletal regenerative medicine. STEM CELLS 2011;29:576–582.

26 Carr MW, Roth SJ, Luther E et al. Monocyte chemoattractant protein 1 acts as a T-lymphocyte chemoattractant. Proc Natl Acad Sci USA 1994;91:3652–3656.

27 Suga H, Glotzbach JP, Sorkin M et al. Paracrine mechanism of angiogenesis in adipose-derived stem cell transplantation. Ann Plast Surg 2014;72:234–241.

28 Miyahara Y, Nagaya N, Kataoka M et al. Monolayered mesenchymal stem cells repair scarred myocardium after myocardial infarction. Nat Med 2006;12:459–465.

29 Galiano RD, Michaels JT, Dobryansky M et al. Quantitative and reproducible murine model of excisional wound healing. Wound Repair Regen 2004;12:485–492.

30 Reinisch A et al. Epigenetic and in vivo comparison of diverse MSC sources reveals an endochondral signature for human hematopoietic niche formation. Blood 2015;125:249–260.

31 Gir P, Oni G, Brown SA et al. Human adipose stem cells: Current clinical applications. Plast Reconstr Surg 2012;129:1277–1290.

32 Glotzbach JP, Wong VW, Gurtner GC et al. Regenerative medicine. Curr Probl Surg 2011;48:148–212.

33 Tsuji W, Rubin JP, Marra KG. Adipose-derived stem cells: Implications in tissue regeneration. World J Stem Cells 2014;6:312–321.

34 Strioga M, Viswanathan S, Darinskas A et al. Same or not the same? Comparison of adipose tissue-derived versus bone marrow-derived mesenchymal stem and stromal cells. Stem Cells Dev 2012;21:2724–2752.

35 Kokai LE, Marra K, Rubin JP. Adipose stem cells: Biology and clinical applications for tissue repair and regeneration. Transl Res 2014;163:399–408.

36 Keck M, Kober J, Riedl O et al. Power assisted liposuction to obtain adipose-derived stem cells: Impact on viability and differentiation to adipocytes in comparison to manual aspiration. J Plast Reconstr Aesthet Surg 2014;67:e1–e8.

37 de Souza Pinto EB, Abdala PC, Maciel CM et al. Liposuction and VASER. Clin Plast Surg 2006;33:107–115.

38 Granéli C, Thorfve A, Ruetschi U et al. Novel markers of osteogenic and adipogenic differentiation of human bone marrow stromal cells identified using a quantitative proteomics approach. Stem Cell Res (Amst) 2014;12:153–165.

See www.StemCellsTM.com for supporting information available online.